

Corrections to the atmospheric neutrino mixing from charged Higgs and W' contribution to ν_τ -nucleon scattering

Ahmed Rashed ^{†‡ 1}, Murugeswaran Duraisamy ^{† 2} and Alakabha Datta ^{† 3}

[†] *Department of Physics and Astronomy,
University of Mississippi,
Lewis Hall, University, MS, 38677, USA.*

[‡] *Department of Physics, Faculty of Science,
Ain Shams University, Cairo, 11566, Egypt.*

(December 2, 2024)

Abstract

We consider charged Higgs and W' gauge boson contributions to the quasielastic scattering $\nu_\tau + n \rightarrow \tau + p$. These effects modify the standard model cross section for this process and thus impact the extraction of the neutrino mixing angle θ_{23} . We include form factor effects in our calculations and find the deviation of the actual mixing angle from the measured one, assuming the standard model cross section, can be significant and can depend on the energy of the neutrino.

¹E-mail: amrashed@olemiss.edu

²E-mail: duraism@phy.olemiss.edu

³E-mail: datta@phy.olemiss.edu

1 Introduction

We now know that neutrinos have masses and there is a leptonic mixing matrix just as there is a quark mixing matrix. This fact has been firmly established through a variety of solar, atmospheric, and terrestrial neutrino oscillation experiments. The next phase in the neutrino physics program is the precision measurement of the mixing angles, finding evidence for CP violation and measuring the absolute masses to resolve the mass hierarchy problem.

The existence of neutrino masses and mixing require physics beyond the standard model (SM). Hence it is not unexpected that neutrinos could have non-standard interactions (NSI). The effects of NSI have been widely considered in neutrino phenomenology [1, 2, 3, 4, 5, 6, 7, 8, 9, 10, 11, 12, 13, 14, 15, 16, 17, 18, 19, 20, 21, 22, 23, 24, 25, 26, 27, 28, 29, 30, 31].

It has been established that NSI cannot be an explanation for the standard oscillation phenomena but it may be present as a subleading effect. Many NSI involve flavor changing neutral current or charged current lepton flavor violating processes. In this paper we consider charged current interactions involving a charged Higgs and a W' gauge boson in the quasielastic scattering process $\nu_\tau + n \rightarrow \tau + p$. In neutrino experiments, to measure the mixing angle the neutrino-nucleus interaction is assumed to be SM like. If there is a charged Higgs or a W' contribution to this interaction then there will be an error in the extracted mixing angle. We will calculate the error in the extracted mixing angle. The above reaction is relevant for experiments like OPERA [32] and ICARUS [33] that seek to measure $\nu_\mu \rightarrow \nu_\tau$ oscillation by the observation of the τ lepton. Some examples of work that deal with NSI at the detector, though not necessarily involving the third family leptons, can be found in Ref. [34, 35, 36].

There are several reasons to consider NSI involving the (ν_τ, τ) sector. First, the third generation may be more sensitive to new physics effects because of their larger masses. As an example, in certain versions of the two Higgs doublet models (2HDM) the couplings of the new Higgs bosons are proportional to the masses and so new physics effects are more pronounced for the third generation. Second, the constraints on new physics (NP) involving the third generation leptons are somewhat weaker allowing for larger new physics effects. Interestingly, the branching ratio of $B \rightarrow \tau\nu_\tau$ shows some tension with the SM predictions [37] and this could indicate NP, possibly in the scalar sector.

If there is NP involving the third generation leptons one can search for it in B decays such as $B \rightarrow \tau\nu_\tau$, $B \rightarrow D^{(*)}\tau\nu_\tau$ [38], $b \rightarrow s\tau^+\tau^-$ e.t.c. In general the NP interaction in B decays may not be related to the one in $\nu_\tau + n \rightarrow \tau + p$ and so this process probes different NP. The same NP in $\nu_\tau + n \rightarrow \tau + p$ can be probed in τ decays [39] and we will consider the constraint on NP from this decay. However, both these processes probe NP in different energy regions. The threshold for τ production in $\nu_\tau + n \rightarrow \tau + p$ is around 3.5 GeV and in fact the OPERA experiment

runs at $E_\nu = 17$ GeV [40] allowing access to larger values for the momentum transfer squared that are not possible in τ decays.

The form of NP in $\nu_\tau + n \rightarrow \tau + p$ involves the operator $\mathcal{O}_{NP} = \bar{u}\Gamma_i d\bar{\tau}\Gamma_j \nu_\tau$, where $\Gamma_{i,j}$ are some Dirac structures. This interaction can also contribute to hadronic tau decays $\tau^- \rightarrow \pi^- \nu_\tau$ and $\tau^- \rightarrow \rho^- \nu_\tau$ and the measured branching ratio of these decays can be used to constrain the couplings in the operator \mathcal{O}_{NP} . The ratio of the charged Higgs contribution to the SM in $\nu_\tau + n \rightarrow \tau + p$ is roughly $\frac{m_N}{m_\pi}$ larger compared to the same ratio in $\tau^- \rightarrow \pi^- \nu_\tau$, where $m_{N,\pi}$ are the nucleon and pion masses. Hence significant charged Higgs effects are possible in $\nu_\tau + n \rightarrow \tau + p$ even after imposing constraints from τ decays. We note that new interaction in the up and down quark sector can be constrained if one assumes CKM unitarity. However we do not consider this constraint as the NP in \mathcal{O}_{NP} involves contribution from both the quark and the lepton sectors.

As noted above, at the quark level NSI in $\nu_\tau + n \rightarrow \tau + p$ involve the u and the d quarks. Often in the analysis of NSI, hadronization effects of the quarks via form factors are not included. As we show in our calculation the form factors play an important role in the energy dependence of the NP effects. In an accurate analysis one should also include nuclear physics effects which take into account the fact that the neutron and the proton are not free but bound in the nucleus. There is a certain amount of model dependence in this part of the analysis [41] and therefore we will not include nuclear effects in our calculation. Such effects can be easily incorporated once the free scattering cross section is known.

The paper is organized in the following way. In the next section, we present a model independent analysis of NP effects. In the following three sections, we consider $\nu_\tau + n \rightarrow \tau + p$ in the SM, in a model with charged Higgs and finally in a model with extra W' gauge boson. In the last section, we present our conclusions.

2 Model independent analysis of new physics

The process $\nu_\tau + n \rightarrow \tau + p$ will impact the measurement of the oscillation probability for $\nu_\mu \rightarrow \nu_\tau$ and hence the extraction of the mixing angle θ_{23} . The measurement of the atmospheric mixing angle θ_{23} relies on the following relationship [42]

$$N(\nu_\tau) = P(\nu_\mu \rightarrow \nu_\tau) \times \Phi(\nu_\mu) \times \sigma_{\text{SM}}(\nu_\tau), \quad (1)$$

where $N(\nu_\tau)$ is the number of observed events, $\Phi(\nu_\mu)$ is the flux of muon neutrinos at the detector, $\sigma^{\text{SM}}(\nu_\tau)$ is the total cross section of tau neutrino interactions with nucleons in the SM at the detector, and $P(\nu_\mu \rightarrow \nu_\tau)$ is the probability for the flavor transition $\nu_\mu \rightarrow \nu_\tau$. This probability is a function of $(E, L, \Delta m_{ij}^2, \theta_{ij})$ with $i, j = 1, 2, 3$ where Δm_{ij}^2 is the squared-mass difference, θ_{ij} is the mixing angle, E is the energy of neutrinos, and L is the distance traveled by neutrinos. The dominant term of the probability is

$$P(\nu_\mu \rightarrow \nu_\tau) \approx \sin^2 2\theta_{23} \cos^4 \theta_{13} \sin^2(\Delta m_{23}^2 L/4E). \quad (2)$$

In the presence of NP, Eq. 1 is modified as

$$N(\nu_\tau) = P(\nu_\mu \rightarrow \nu_\tau) \times \Phi(\nu_\mu) \times \sigma_{\text{tot}}(\nu_\tau), \quad (3)$$

with $\sigma_{\text{tot}}(\nu_\tau) = \sigma_{\text{SM}}(\nu_\tau) + \sigma_{\text{NP}}(\nu_\tau)$ where $\sigma_{\text{NP}}(\nu_\tau)$ refers to the additional terms to the SM contribution towards the total cross section. Hence, $\sigma_{\text{NP}}(\nu_\tau)$ includes contributions from both the SM and NP interference amplitude, and the pure NP amplitude. From Eqs. (1, 3), assuming θ_{13} to be small⁴

$$\sin^2 2(\theta_{23})_{ac} = \sin^2 2(\theta_{23})_{SM} \frac{1}{1 + r_{23}}, \quad (4)$$

where $(\theta_{23})_{ac} = (\theta_{23})_{SM} + \delta_{23}$ is the actual atmospheric mixing angle, and the best-fit value for the mixing angle is given by $\theta_{23} = 42.8^\circ$ [43]. The relation between the ratio of the NP contribution to the SM cross section $r_{23} = \frac{\sigma_{\text{NP}}}{\sigma_{\text{SM}}}$ and δ_{23} can be expressed in a model independent form as

$$r_{23} = \left[\frac{\sin 2(\theta_{23})_{SM}}{\sin 2((\theta_{23})_{SM} + \delta_{23})} \right]^2 - 1. \quad (5)$$

Fig. 1 shows the correlation between $r_{23}\%$ and δ_{23} [Deg]. One can see that $\delta_{23} \sim -5^\circ$ requires $r_{23} \sim 5\%$. In the following sections, we consider specific models of NP to calculate r_{23} . We will consider a model with a charged Higgs and a W' model with both left and right handed couplings.

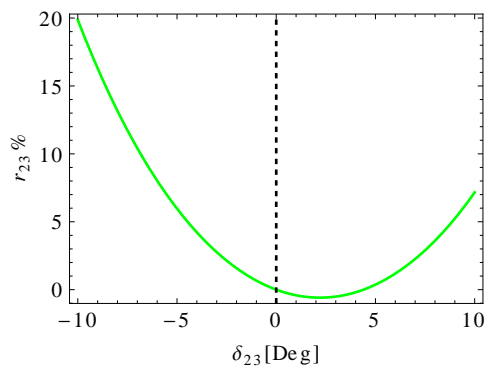


Figure 1: Correlation plot for $r_{23} = \sigma_{\text{NP}}/\sigma_{\text{SM}}\%$ and $\delta_{23}[\text{Deg}]$.

⁴ There is recent evidence of a non-zero θ_{13} [44]. The presence of NP impacts the extraction of the combination $\sin^2 2\theta_{23} \cos^4 \theta_{13}$. We assume that NP only changes the extracted value of θ_{23} .

3 Quasielastic neutrino scattering off free nucleon -SM

In this section, we summarize the SM results for the quasielastic scattering of a neutrino on a free neutron target

$$\nu_l(k) + n(p) \rightarrow l(k') + p(p'), \quad (6)$$

where $k, k', p,$ and p' denote the four-momenta and l indicates the lepton e, μ or τ . The spin averaged matrix element squared for the above reaction is a convolution of spin-averaged leptonic and hadronic tensors $L^{\mu\nu}$ and $H^{\mu\nu}$:

$$|\bar{\mathcal{M}}|^2 = \frac{G_F^2}{2} L^{\mu\nu} H_{\mu\nu}. \quad (7)$$

The leptonic tensor calculation is straight forward but the hadronic tensor involves non-perturbative effects. In order to calculate the hadronic tensor, we define the charged hadronic current for this process;

$$\langle p(p') | J_\mu | n(p) \rangle = V_{ud} \langle p(p') | (V_\mu - A_\mu) | n(p) \rangle. \quad (8)$$

The expressions for the matrix elements of the vector and axial vector currents are summarized in terms of six form factors in the appendix. Due to time reversal invariance, the form factors are real functions of $t = q^2$. When invariance under charge conjugation holds, two form factors vanish ($F_S = 0, F_T = 0$) [45]. The matrix element, then, can be written as

$$\begin{aligned} \mathcal{M} = & \frac{G \cos \theta_c}{\sqrt{2}} \bar{u}_l(k') \gamma^\mu (1 - \gamma_5) u_{\nu_l}(k) \\ & \bar{u}_{N'}(p') \left[F_1^V(t) \gamma_\mu + F_2^V(t) i \frac{\sigma_{\mu\nu} q^\nu}{2M} + F_A(t) \gamma_\mu \gamma_5 + F_P(t) \gamma_5 \frac{q_\mu}{M} \right] u_N(p), \end{aligned} \quad (9)$$

where N and N' are the initial and final nucleon while l and ν_l are the final charged lepton and the initial neutrino. In our case $N = n, N' = p, l = \tau,$ and $\nu_l = \nu_\tau$.

After evaluating $|\bar{\mathcal{M}}|^2$, one can obtain the SM differential cross section for the reaction in Eq. (6) [45]

$$\frac{d\sigma_{SM}}{dt} = \frac{M^2 G_F^2 \cos^2 \theta_c}{8\pi E_\nu^2 (1 - t/m_W^2)^2} \left[A_{SM} + B_{SM} \frac{(s-u)}{M^2} + C_{SM} \frac{(s-u)^2}{M^4} \right], \quad (10)$$

where $G_F = 1.116637 \times 10^{-5} \text{ GeV}^{-2}$ is the Fermi coupling constant, $\cos \theta_c = 0.9746$ is the cosine of the Cabbibo angle, m_W is the W boson mass, E_ν is the incident neutrino energy. $M = (M_p + M_n)/2 \approx 938.9 \text{ MeV}$ is the nucleon mass and we neglect the proton-neutron mass difference. The expressions for the coefficients f_{SM} ($f = A, B, C$) are summarized in the appendix. The Mandelstam variables are defined by $s = (k + p)^2, t = q^2 = (k - k')^2,$ and $u = (k - p')^2$. The expressions for these variables in terms of E_ν and the lepton energy E_l are given in the appendix.

4 Quasielastic neutrino scattering off free nucleon - Charged Higgs Effect

In this section we consider the charged Higgs contribution to $\nu_\tau + n \rightarrow \tau + p$. Charged Higgs particles appear in multi-Higgs models. In the SM the Higgs couples to the fermion masses but in a general multi-Higgs model the charged Higgs may not couple to the mass. What is true in most models is the coupling of the charged Higgs to the leptons is no longer universal. Hence the extraction of θ_{23} from $\nu_\mu \rightarrow \nu_\mu$ survival probability will be different from $\nu_\mu \rightarrow \nu_\tau$ probability in the presence of a charged Higgs effect.

The most general coupling of the charged Higgs is,

$$\mathcal{L} = \frac{g}{2\sqrt{2}} \left[V_{u_i d_j} \bar{u}_i (g_S^{u_i d_j} + g_P^{u_i d_j} \gamma^5) d_j + \bar{\nu}_i (g_S^{\nu_i l_j} + g_P^{\nu_i l_j} \gamma^5) l_j \right] H^+, \quad (11)$$

where u_i and d_j refer to up and down type quarks, and ν_i and l_j refer to neutrinos and charged leptons. The other parameters $g = e/\sin\theta_W$ is the SM weak coupling constant, $V_{u_i d_j}$ is the CKM matrix element, and $g_{S,P}$ are the scalar and pseudo-scalar couplings of charged Higgs to fermions.

We will choose the couplings $g_{S,P}$, relevant for $\nu_\tau + n \rightarrow \tau + p$, to be given by the two Higgs doublet model of type II (2HDM II). However to keep things general we will not assume any relation between these couplings and the couplings in other sectors. To constrain the couplings $g_{S,P}$ we will only consider processes that are generated by $\mathcal{O}_{NP} = \bar{u}\Gamma_i d \bar{\tau}\Gamma_j \nu_\tau$. In the 2HDM II, model constraints on the model parameters come from various sectors [46]. These constraints turn out to be similar but slightly stronger than the ones obtained in our analysis.

The coupling of charged Higgs boson (H^+) interactions to SM fermion in the 2HDM II is [47]

$$\begin{aligned} \mathcal{L} = \frac{g}{2\sqrt{2}M_W} \sum_{ij} & \left[m_{u_i} \cot\beta \bar{u}_i V_{ij} P_L d_j + m_{d_j} \tan\beta \bar{u}_i V_{ij} P_R d_j \right. \\ & \left. + m_{l_j} \tan\beta \bar{\nu}_i P_R l_j \right] H^+, \end{aligned} \quad (12)$$

where $P_{L,R} = \frac{(1\mp\gamma^5)}{2}$, and $\tan\beta$ is the ratio between the two v.e.v's of the two Higgs doublets. Comparing Eq. (11) and Eq. (12), one can obtain

$$\begin{aligned} g_S^{u_i d_j} &= \left(\frac{m_{d_j} \tan\beta + m_{u_i} \cot\beta}{m_W} \right), \\ g_P^{u_i d_j} &= \left(\frac{m_{d_j} \tan\beta - m_{u_i} \cot\beta}{m_W} \right), \\ g_S^{\nu_i l_j} &= g_P^{\nu_i l_j} = \frac{m_{l_j} \tan\beta}{m_W}. \end{aligned} \quad (13)$$

Constraints on the size of the operator $\mathcal{O}_{NP} = \bar{u}\Gamma_i d\bar{\tau}\Gamma_j\nu_\tau$ can be obtained from the branching ratio of the decay $\tau^- \rightarrow \pi^-\nu_\tau$. In the presence of a charged Higgs, the branching ratio for this process is

$$Br_{\tau^- \rightarrow \pi^-\nu_\tau}^{SM+H} = Br_{\tau^- \rightarrow \pi^-\nu_\tau}^{SM} (1 + r_H^\pi)^2, \quad (14)$$

where the charged Higgs contribution is

$$r_H^\pi = \left(\frac{m_u - m_d \tan^2 \beta}{m_u + m_d} \right) \frac{m_\pi^2}{m_H^2}, \quad (15)$$

and the SM branching ratio is related to the tau lepton width (Γ_τ) and the decay rate ($\Gamma_{\tau^- \rightarrow \pi^-\nu_\tau}^{SM}$) as $Br_{\tau^- \rightarrow \pi^-\nu_\tau}^{SM} = \Gamma_{\tau^- \rightarrow \pi^-\nu_\tau}^{SM} / \Gamma_\tau$ with

$$\Gamma_{\tau^- \rightarrow \pi^-\nu_\tau}^{SM} = \frac{G_F^2}{16\pi} |V_{ud}|^2 f_\pi^2 m_\tau^3 \left(1 - \frac{m_\pi^2}{m_\tau^2}\right)^2 \delta_{\tau/\pi}. \quad (16)$$

Here $\delta_{\tau/\pi} = 1.0016 \pm 0.0014$ [48] is the radiative correction. Further, the SM branching ratio can be also expressed as [49]

$$Br_{\tau^- \rightarrow \pi^-\nu_\tau}^{SM} = 0.607 Br(\tau^- \rightarrow \nu_\tau e^- \bar{\nu}_e) = 10.82 \pm .02\%, \quad (17)$$

while the measured $Br(\tau^- \rightarrow \pi^-\nu_\tau)_{exp} = (10.91 \pm 0.07)\%$ [50]. In Fig. 2 we show the constraints on $m_H - \tan \beta$ from $\tau^- \rightarrow \pi^-\nu_\tau$.

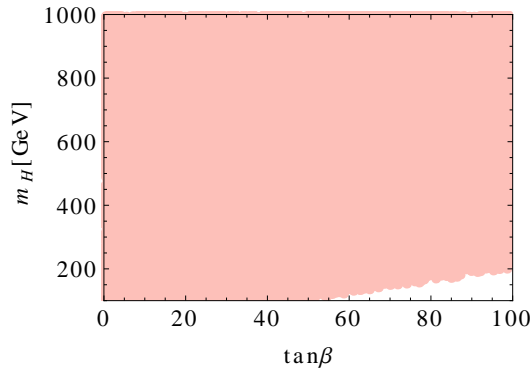


Figure 2: Constraint by $Br(\tau^- \rightarrow \pi^-\nu_\tau)$ at 95 % CL. The colored region is allowed.

Finally, we note that τ has a significant branching ratio to $\tau^- \rightarrow \rho^-\nu_\tau$ [50]. However a charged Higgs cannot contribute to this decay and hence there is no constraint on the charged Higgs couplings from this decay [39].

Keeping in mind the constraints from Fig. (2) we calculate the charged Higgs contribution to $\nu_\tau + n \rightarrow \tau + p$. The modified differential cross section for the reaction Eq. (6) is

$$\frac{d\sigma_{SM+H}}{dt} = \frac{M^2 G_F^2 \cos^2 \theta_c}{8\pi E_\nu^2 (1 - t/m_W^2)^2} \left[A_H + B_H \frac{(s-u)}{M^2} + C_{SM} \frac{(s-u)^2}{M^4} \right], \quad (18)$$

where $x_H = m_W^2/M_H^2$, $A_H = A_{SM} + 2x_H \text{Re}(A_H^I) + x_H^2 A_H^P$, and $B_H = B_{SM} + 2x_H \text{Re}(B_H^I)$. Superscripts I and P denote the SM-Higgs interference and pure Higgs contributions, respectively. The expressions for the quantities $A_H^{I,P}$ and B_H^I are given in the appendix. The terms A_H^I and B_H^I are proportional to the tiny neutrino mass and we will ignore them in our calculation. Note that this happens because we have chosen the couplings to be given by the 2HDM II. With general couplings of the charged Higgs these interference terms will be present. The charged Higgs contribution relative to the SM $r_H = \frac{\sigma_H}{\sigma_{SM}}$ is proportional to t because of the dominant term $x_t G_P^2$, where $x_t = t/4M^2$ (see appendix for more details). Consequently, r_H is proportional to the incident neutrino energy (see Fig. (3)). We find $r_H \sim 9\%$ at $M_H = 200$ GeV for $E_\nu = 17$ GeV.

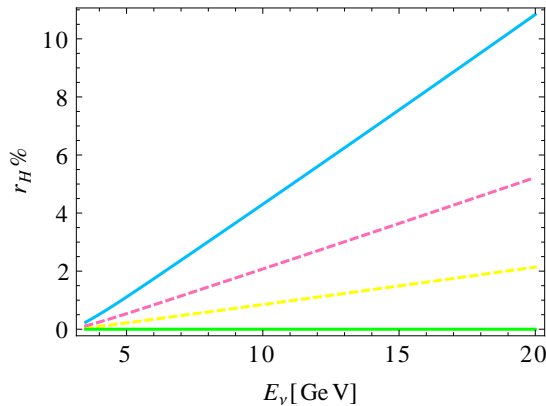


Figure 3: The figure illustrates variation of $r_H\%$ with E_ν . The green line corresponds to SM prediction. The yellow, pink, and blue lines correspond to $\tan\beta = 40, 50, 60$, respectively at $M_H = 200$ GeV.

The deviation δ_{23} is negative as there is no interference with the SM and hence the cross-section for $\nu_\tau + n \rightarrow \tau + p$ is always larger than the SM cross-section. This means, if the true θ_{23} is close to maximal then experiments should measure θ_{23} larger than the maximal value in the presence of a charged Higgs contribution. The Higgs contribution can enhance δ_{23} up to -6° at $M_H = 200$ GeV for $E_\nu = 17$ GeV.

5 Quasielastic neutrino scattering off free nucleon- W' model

Many extensions of the SM contain a W' gauge boson. We next consider modification to $\nu_\tau + n \rightarrow \tau + p$ in models with a W' . There are limits on the W' mass from direct searches to final states involving an electron and muon assuming SM couplings for the W' [50]. These limits generally do not apply to the W' coupling to ν_τ and τ which is relevant for our calculation.

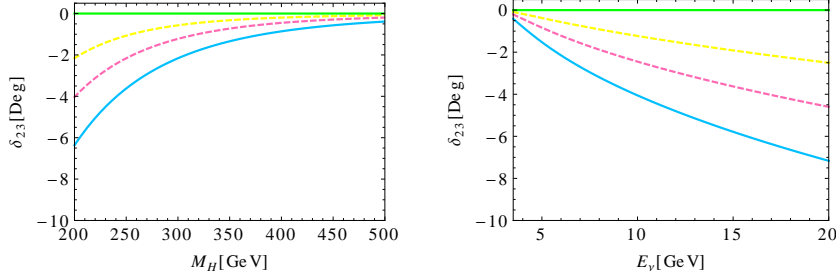


Figure 4: The figure illustrates variation of δ_{23} with M_H and E_ν . The green line corresponds to SM prediction. The yellow, pink, and blue lines correspond to $\tan\beta = 40, 50, 60$. The left figure is evaluated at $E_\nu = 17$ GeV, while the right figure at $M_H = 200$ GeV. Here, we use the best-fit value $\theta_{23} = 42.8^\circ$ [43].

The lowest dimension effective Lagrangian of W' interactions to the SM fermions has the form

$$\mathcal{L} = \frac{g}{\sqrt{2}} V_{f'f} \bar{f}' \gamma^\mu (g_L^{f'f} P_L + g_R^{f'f} P_R) f W'_\mu + h.c., \quad (19)$$

where f' and f refer to the fermions and $g_{L,R}^{f'f}$ are the left and the right handed couplings of the W' . For a SM-like W' boson $g_L^{f'f} = 1$ and $g_R^{f'f} = 0$. We will assume $g_{L,R}^{f'f}$ to be real. Constraints on the couplings in Eq. (19) come from the hadronic τ decays. We will consider constraints from the decays $\tau^- \rightarrow \pi^- \nu_\tau$ and $\tau^- \rightarrow \rho^- \nu_\tau$.

The branching ratio for $\tau^- \rightarrow \pi^- \nu_\tau$ is

$$Br_{\tau^- \rightarrow \pi^- \nu_\tau}^{SM+W'} = Br_{\tau^- \rightarrow \pi^- \nu_\tau}^{SM} (1 + r_{W'}^\pi)^2, \quad (20)$$

where the W' contribution is

$$r_{W'}^\pi = x_{W'} g_L^{\tau\nu} (g_L^{ud} - g_R^{ud}), \quad (21)$$

and $x_{W'} = m_{W'}^2/M_{W'}^2$. The branching ratio for the $\tau^- \rightarrow \rho^- \nu_\tau$ process is

$$Br_{\tau^- \rightarrow \rho^- \nu_\tau}^{SM+W'} = Br_{\tau^- \rightarrow \rho^- \nu_\tau}^{SM} (1 + r_{W'}^\rho)^2, \quad (22)$$

with W' contribution

$$r_{W'}^\rho = x_{W'} g_L^{\tau\nu} (g_L^{ud} + g_R^{ud}). \quad (23)$$

The SM branching ratio is related to decay rate as $Br_{\tau^- \rightarrow \rho^- \nu_\tau}^{SM} = \Gamma_{\tau^- \rightarrow \rho^- \nu_\tau}^{SM} / \Gamma_\tau$ with

$$\Gamma_{\tau^- \rightarrow \rho^- \nu_\tau}^{SM} = \frac{G_F^2}{16\pi} |V_{ud}|^2 f_\rho^2 m_\tau^3 \left(1 - \frac{m_\rho^2}{m_\tau^2}\right)^2 \left(1 + \frac{2m_\rho^2}{m_\tau^2}\right), \quad (24)$$

where $f_\rho = 223$ MeV [51]. Further, the SM branching ratio can be also expressed as [49]

$$Br_{\tau^- \rightarrow \rho^- \nu_\tau}^{SM} = 1.23 Br(\tau^- \rightarrow \nu_\tau e^- \bar{\nu}_e) = 21.92 \pm 0.05\%. \quad (25)$$

The measured branching ratio is $Br(\tau^- \rightarrow \rho^- \nu_\tau)_{exp} = (23.1 \pm 0.98)\%$ [50].

Fig. (5) and Fig. (6) show the allowed regions for the W' couplings. The couplings are uniformly varied between $[-2, 2]$ and constrained by the measured $\tau^- \rightarrow \pi^- \nu_\tau$ and $\tau^- \rightarrow \rho^- \nu_\tau$ branching ratios with one sigma errors.

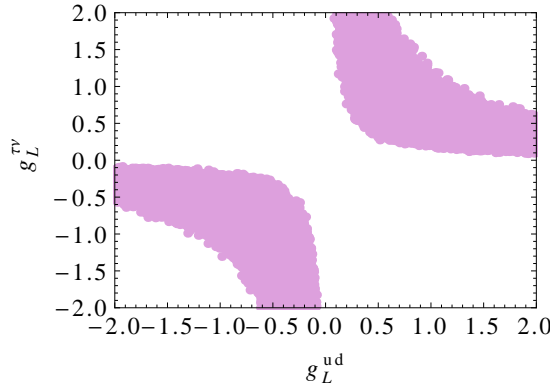


Figure 5: The constraints on the W' couplings without right handed coupling. The constraints are from $\tau^- \rightarrow \pi^- \nu_\tau$ and $\tau^- \rightarrow \rho^- \nu_\tau$ branching ratios. The errors in the branching ratios are varied within 1σ . The colored regions are allowed.

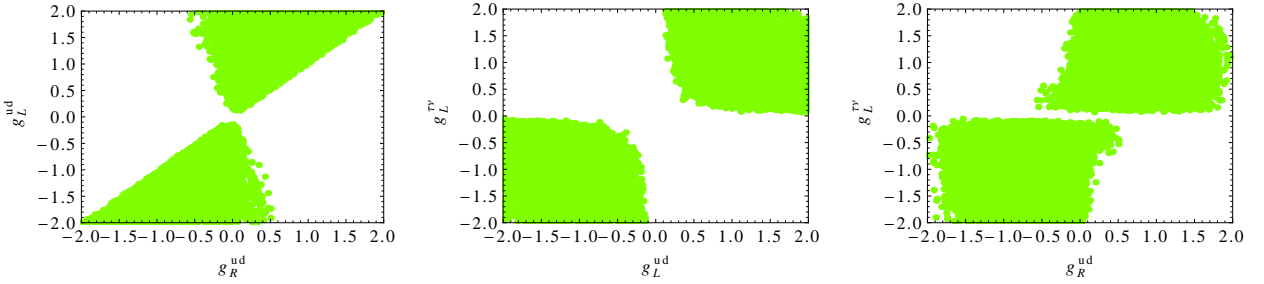


Figure 6: The constraints on the W' couplings with both left and right handed couplings. The constraints are from $\tau^- \rightarrow \pi^- \nu_\tau$ and $\tau^- \rightarrow \rho^- \nu_\tau$ branching ratios. The errors in the branching ratios are varied within 1σ . The colored regions are allowed.

In the presence of the W' gauge boson, we can obtain the modified differential cross section for the reaction Eq. (6) as

$$\frac{d\sigma_{SM+W'}}{dt} = \frac{M^2 G_F^2 \cos^2 \theta_c}{8\pi E_\nu^2 (1 - t/m_W^2)^2} \left[A' + B' \frac{(s-u)}{M^2} + C' \frac{(s-u)^2}{M^4} \right], \quad (26)$$

where the coefficients A', B', C' include both the SM and W' contributions. The expressions for these coefficients are given in the appendix.

For SM-like W' boson, with right-handed couplings ignored, the structure of the differential cross section is similar to the one in the SM case. Hence, W' contribution relative to the SM $r_{W'} = \frac{\sigma_{W'}}{\sigma_{SM}}$ does not depend on the incident neutrino energy E_ν . We find, $r_{W'} \sim 5\%$ at $M_{W'} = 500$ GeV from the hadronic tau decay constraints in Fig. (5). The variation of δ_{23} with the W' mass is shown in Fig. (7). In this case, δ_{23} is always negative and can reach up to -5° at $M_{W'} = 500$ GeV. Note that, δ_{23} also does not dependent on E_ν .

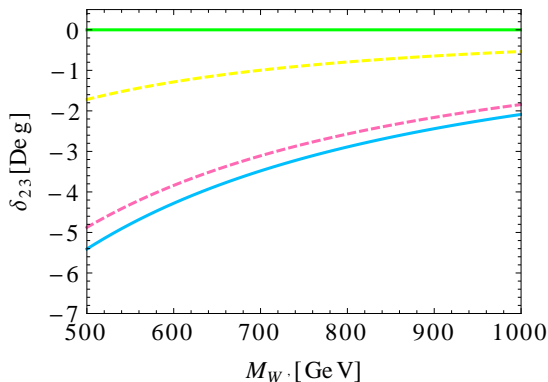


Figure 7: The figure illustrates the deviation δ_{23} with the W' mass when only left-handed couplings are present. The lines show predictions for some representative values of W' couplings ($g_L^{\tau\nu\tau}, g_L^{ud}$) in Fig. (5). The green line corresponds to the SM prediction, and the blue line to $(-0.33, -1.13)$ at $E_\nu = 17$ GeV. Here, we use the best-fit value $\theta_{23} = 42.8^\circ$ [43].

Next, we consider the right-handed couplings also. The differential cross section in this case is shown in Fig. (8). The total differential cross section differs appreciably from the SM at low t . We find that $r_{W'}$ depends slightly on the neutrino energy and $r_{W'}$ can be $\sim 18\%$ at $M_{W'} = 500$ GeV for $E_\nu = 17$ GeV. The variation of δ_{23} with the W' mass and E_ν are shown in Figs. (9). In this case, δ_{23} is mostly negative and can reach up to -10° at $M_{W'} = 500$ GeV for $E_\nu = 17$ GeV.

6 Conclusion

In this paper we calculated the effect of a charged Higgs and a W' contribution to $\nu_\tau + n \rightarrow \tau + p$. We constrained the parameters of both the models from $\tau^- \rightarrow \pi^- \nu_\tau$ and $\tau^- \rightarrow \rho^- \nu_\tau$ decays. Corrections to the SM contribution to $\nu_\tau + n \rightarrow \tau + p$ impact the extraction of the neutrino atmospheric mixing angle θ_{23} . We found that both models can produce significant corrections to δ_{23} that measures the deviation of the actual θ_{23} from the measured θ_{23} . When a charged Higgs is involved δ_{23} is negative.

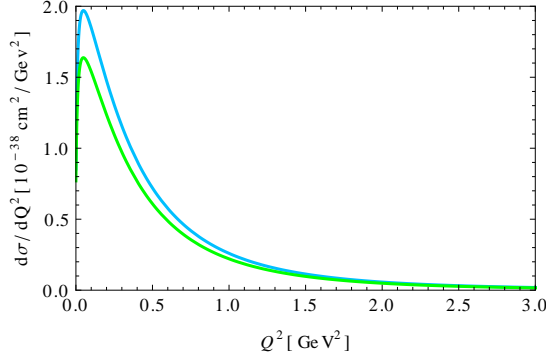


Figure 8: The differential cross section for $\nu_\tau + n \rightarrow \tau + p$ with both left and right handed W' couplings. The blue line shows prediction for some representative values of W' couplings $(g_L^{\tau\nu\tau}, g_L^{ud}, g_R^{ud}) = (-1.8, -1.95, 0.90)$ at $M_{W'} = 516$ GeV, that are consistent with the constraints in Fig. (6), at $E_\nu = 17$ GeV. The green line corresponds to SM prediction.

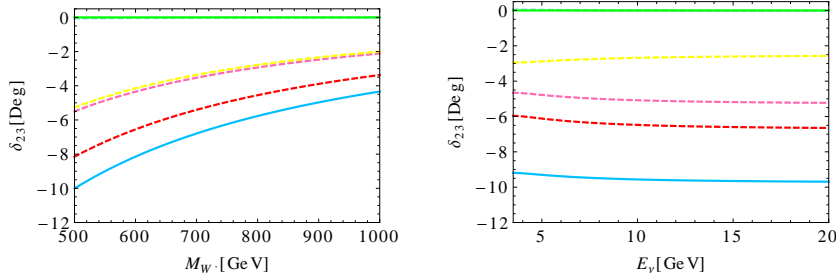


Figure 9: The left (right) panel figures illustrate the deviation δ_{23} with the W' mass (E_ν) when both left and right-handed W' couplings are present. The lines show predictions for some representative values of the W' couplings $(g_L^{\tau\nu\tau}, g_L^{ud}, g_R^{ud})$ taken from Fig. (6). The green line corresponds to the SM prediction. The blue line in the left figure corresponds to $(-1.8, -1.95, 0.90)$ at $E_\nu = 17$ GeV, and the blue line in the right figure corresponds to $M_{W'} = 516$ GeV. Here, we use the best-fit value $\theta_{23} = 42.8^\circ$ [43].

This is because there is no interference of the charged Higgs contribution with the SM and so the cross section for $\nu_\tau + n \rightarrow \tau + p$ is always larger than the SM cross section. This means, if the true θ_{23} is close to maximal then experiments should measure θ_{23} larger than the maximal value in the presence of a charged Higgs contribution. In this case we also found δ_{23} to increase in magnitude with the neutrino energy. Hence a possible sign of charged Higgs effect would be a measurement of θ_{23} that shows an increase with increasing neutrino energy. For the W' model we calculated significant contribution to δ_{23} which can be both positive and negative, but is mostly negative. The deviation δ_{23} was found to be independent of the neutrino energy for a

left handed W' but neutrino energy dependent when both left and right handed W' chiralities were present. We have presented in this paper a first estimation of charged Higgs and W' effects in the extraction of θ_{23} . We hope more detailed calculations including nuclear as well as detector effects will be done to find out whether these new physics effects can be observed at present ν_τ appearance experiments and/or to motivate new experiments that can detect these effects.

Acknowledgements

We thank Sandip Pakvasa and Nita Sinha for useful discussion. This work was financially supported by the US-Egypt Joint Board on Scientific and Technological Co-operation award (Project ID: 1855) administered by the US Department of Agriculture and in part by the National Science Foundation under Grant No. NSF PHY-1068052.

Appendix

Hadronic form factors

The expressions for the vector and axial vector hadronic matrix element are

$$\begin{aligned} \langle p(p') | V_\mu | n(p) \rangle &= \bar{u}_p(p') \left[\gamma_\mu F_1^V + \frac{i}{2M} \sigma_{\mu\nu} q^\nu F_2^V + \frac{q_\mu}{M} F_S \right] u_n(p), \\ -\langle p(p') | A_\mu | n(p) \rangle &= \bar{u}_p(p') \left[\gamma_\mu F_A + \frac{i}{2M} \sigma_{\mu\nu} q^\nu F_T + \frac{q_\mu}{M} F_P \right] \gamma_5 u_n(p). \end{aligned} \quad (27)$$

Here $q = p' - p$ and the form factors F_i are functions of $t = q^2$. The parametrization of the axial vector and pseudoscalar form factors are [45]:

$$\begin{aligned} F_A(t) &= F_A(0) \left(1 - \frac{t}{M_A^2} \right)^{-2}, \\ F_P(t) &= \frac{2M^2 F_A(0)}{m_\pi^2 - t}, \end{aligned} \quad (28)$$

where $F_A(0) = -1.2695$ is the axial coupling [50], m_π is the charged pion mass, and $M_A = 1.35$ GeV is the axial-vector mass [52]. The expression for $F_P(t)$ can be shown to be true at low energy where the predictions of chiral perturbation theory are valid [53]. We have assumed the relation to hold at high t also. Note that $F_A(0)$ is sometimes replaced by $F_A(t)$ which gives similar results for $F_P(t)$ at low t but very different results at high t .

The Dirac and Pauli form factors $F_{1,2}^V$ are

$$F_1^V(t) = \frac{G_E(t) - x_t G_M(t)}{1 - x_t}, \quad F_2^V(t) = \frac{G_M(t) - G_E(t)}{1 - x_t}, \quad (29)$$

where $x_t = t/4M^2$ and

$$G_M = G_M^p - G_M^n, \quad G_E = G_E^p - G_E^n. \quad (30)$$

Here $G_E^{p,n}$ and $G_M^{p,n}$ are the elastic electric and magnetic form factors of the proton and neutron, respectively. The simplest parametrization of these form factor are given by the dipole approximation

$$G_E^p \approx G_D, \quad G_E^n \approx 0, \quad G_M^p \approx \mu_p G_D, \quad G_M^n \approx \mu_n G_D, \quad (31)$$

where $G_D = (1 - t/M_V^2)^{-2}$, $M_V = 0.843$ GeV is the vector mass, and $\mu_p(\mu_n)$ is the anomalous magnetic moment of the proton (neutron) [54]. Applying the equation of motion, one can obtain the hadronic matrix elements for the scalar and pseudoscalar currents

$$\begin{aligned} \langle p(p') | \bar{u}d | n(p) \rangle &= \bar{p}(p_4) G_S n(p_2), \\ -\langle p(p') | \bar{u}\gamma_5 d | n(p) \rangle &= \bar{p}(p_4) G_P \gamma_5 n(p_2), \end{aligned} \quad (32)$$

where

$$\begin{aligned} G_S(t) &= r_N F_1^V(t), \quad \text{with } r_N = \frac{M_n - M_p}{(m_d - m_u)} \sim \mathcal{O}(1), \\ G_P(t) &= \frac{M[F_A(t) + 2x_t F_P(t)]}{\bar{m}_q}, \end{aligned} \quad (33)$$

with $\bar{m}_q = (m_u + m_d)/2$.

Kinematic details

The Mandelstam variables in terms of E_ν and the lepton energy E_l are

$$\begin{aligned} s &= M^2 + 2ME_\nu, \quad t = 2M(E_l - E_\nu), \\ s - u &= 4ME_\nu + t - m_l^2. \end{aligned} \quad (34)$$

Then t and E_l lie in the intervals

$$m_l^2 - 2E_\nu^{\text{cm}}(E_l^{\text{cm}} + p_l^{\text{cm}}) \leq t \leq m_l^2 - 2E_\nu^{\text{cm}}(E_l^{\text{cm}} - p_l^{\text{cm}}), \quad (35)$$

$$E_\nu + \frac{m_l^2 - 2E_\nu^{\text{cm}}(E_l^{\text{cm}} + p_l^{\text{cm}})}{2M} \leq E_l \leq E_\nu + \frac{m_l^2 - 2E_\nu^{\text{cm}}(E_l^{\text{cm}} - p_l^{\text{cm}})}{2M}, \quad (36)$$

where the energy and momentum of the lepton and the neutrino in the center of mass (cm) system are

$$\begin{aligned} E_\nu^{\text{cm}} &= \frac{(s - M^2)}{2\sqrt{s}}, \quad p_l^{\text{cm}} = \sqrt{(E_l^{\text{cm}})^2 - m_l^2}, \\ E_l^{\text{cm}} &= \frac{(s - M^2 + m_l^2)}{2\sqrt{s}}. \end{aligned} \quad (37)$$

The threshold neutrino energy to create the charged lepton partner is given by

$$E_{\nu_l}^{\text{th}} = \frac{(m_l + M_p)^2 - M_n^2}{2M_n}, \quad (38)$$

where m_l , M_p , M_n are the masses of the charged lepton, proton, and neutron, respectively. In our case, the threshold energy of tau neutrino is $E_{\nu_\tau}^{\text{th}} = 3.45$ GeV.

The differential cross section in the laboratory frame is given by

$$\frac{d\sigma_{\text{tot}}(\nu_l)}{dt} = \frac{|\bar{\mathcal{M}}|^2}{64\pi E_\nu^2 M^2 (1 - t/m_W^2)^2}. \quad (39)$$

The expressions for the coefficients f_{SM} ($f = A, B, C$) in the SM differential cross section (see Eq.(10)) are

$$\begin{aligned} A_{SM} &= 4(x_t - x_l) \left[(F_1^V)^2 (1 + x_l + x_t) + (F_A)^2 (-1 + x_l + x_t) + (F_2^V)^2 (x_l + x_t^2 + x_t) \right. \\ &\quad \left. + 4F_P^2 x_l x_t + 2F_1^V F_2^V (x_l + 2x_t) + 4F_A F_P x_l \right], \\ B_{SM} &= 4x_t F_A (F_1^V + F_2^V), \\ C_{SM} &= \frac{(F_1^V)^2 + F_A^2 - x_t (F_2^V)^2}{4}, \end{aligned} \quad (40)$$

where $x_l = m_l^2/4M^2$.

The expressions for the quantities $A_H^{I,P}$ and B_H^I in the differential cross section in Eq. (18) are

$$\begin{aligned} A_H^I &= 2\sqrt{x_l}(x_t - x_l)g_P^{ud}(g_S^{l\nu_l} - g_P^{l\nu_l})G_P(F_A + 2F_P x_t), \\ B_H^I &= \frac{1}{2}\sqrt{x_l}g_S^{ud}(g_S^{l\nu_l} - g_P^{l\nu_l})G_S(F_1^V + F_2^V x_t), \\ A_H^P &= 2(x_t - x_l)(|g_S^{l\nu_l}|^2 + |g_P^{l\nu_l}|^2)(|g_P^{ud}|^2 G_P^2 x_t + |g_S^{ud}|^2 G_S^2 (x_t - 1)). \end{aligned} \quad (41)$$

For the 2HDM II model couplings, $g_{S,P}$ are given in Eq. (13). Note that, the interference terms A_H^I and B_H^I vanish in this model.

The expressions for the quantities f' ($f = A, B, C$) in the differential cross section in Eq. (26) are

$$\begin{aligned} A' &= 4(x_t - x_l) \left[(1 + r_{W'}^\rho)^2 \left((F_1^V)^2 (1 + x_l + x_t) + 2F_1^V F_2^V (x_l + 2x_t) + (F_2^V)^2 (x_l + x_t^2 + x_t) \right) \right. \\ &\quad \left. + (1 + r_{W'}^\pi)^2 \left((F_A)^2 (-1 + x_l + x_t) + 4F_A F_P x_l + 4F_P^2 x_l x_t \right) \right], \\ B' &= 4Re[(1 + r_{W'}^\rho)(1 + r_{W'}^{\pi*})]x_t F_A (F_1^V + F_2^V), \\ C' &= \frac{1}{4} \left[(1 + r_{W'}^\rho)^2 ((F_1^V)^2 - x_t (F_2^V)^2) + (1 + r_{W'}^\pi)^2 F_A^2 \right]. \end{aligned} \quad (42)$$

In the absence of W' contributions, f' 's reduce to the respective SM results in Eq. 40.

References

- [1] L. Wolfenstein, Phys. Rev. D **17**, 2369 (1978).
- [2] S. P. Mikheev and A. Y. Smirnov, Sov. J. Nucl. Phys. **42**, 913 (1985) [Yad. Fiz. **42**, 1441 (1985)].
- [3] E. Roulet, Phys. Rev. D **44**, 935 (1991).
- [4] G. Brooijmans, hep-ph/9808498.
- [5] M. C. Gonzalez-Garcia, M. M. Guzzo, P. I. Krastev, H. Nunokawa, O. L. G. Peres, V. Pleitez, J. W. F. Valle and R. Zukanovich Funchal, Phys. Rev. Lett. **82**, 3202 (1999) [hep-ph/9809531].
- [6] M. M. Guzzo, A. Masiero and S. T. Petcov, Phys. Lett. B **260**, 154 (1991).
- [7] S. Bergmann, M. M. Guzzo, P. C. de Holanda, P. I. Krastev and H. Nunokawa, Phys. Rev. D **62**, 073001 (2000) [hep-ph/0004049].
- [8] M. M. Guzzo, H. Nunokawa, P. C. de Holanda and O. L. G. Peres, Phys. Rev. D **64**, 097301 (2001) [hep-ph/0012089].
- [9] M. Guzzo, P. C. de Holanda, M. Maltoni, H. Nunokawa, M. A. Tortola and J. W. F. Valle, Nucl. Phys. B **629**, 479 (2002) [hep-ph/0112310].
- [10] Y. Grossman, Phys. Lett. B **359**, 141 (1995) [hep-ph/9507344].
- [11] T. Ota and J. Sato, Phys. Lett. B **545**, 367 (2002) [hep-ph/0202145].
- [12] A. Friedland and C. Lunardini, Phys. Rev. D **72**, 053009 (2005) [hep-ph/0506143].
- [13] N. Kitazawa, H. Sugiyama and O. Yasuda, hep-ph/0606013.
- [14] A. Friedland and C. Lunardini, Phys. Rev. D **74**, 033012 (2006) [hep-ph/0606101].
- [15] M. Blennow, T. Ohlsson and J. Skrotzki, Phys. Lett. B **660**, 522 (2008) [hep-ph/0702059 [HEP-PH]].
- [16] A. Esteban-Pretel, J. W. F. Valle and P. Huber, Phys. Lett. B **668**, 197 (2008) [arXiv:0803.1790 [hep-ph]].
- [17] M. Blennow, D. Meloni, T. Ohlsson, F. Terranova and M. Westerberg, Eur. Phys. J. C **56**, 529 (2008) [arXiv:0804.2744 [hep-ph]].

- [18] M. C. Gonzalez-Garcia, Y. Grossman, A. Gusso and Y. Nir, Phys. Rev. D **64**, 096006 (2001) [hep-ph/0105159].
- [19] A. M. Gago, M. M. Guzzo, H. Nunokawa, W. J. C. Teves and R. Zukanovich Funchal, Phys. Rev. D **64**, 073003 (2001) [hep-ph/0105196].
- [20] P. Huber and J. W. F. Valle, Phys. Lett. B **523**, 151 (2001) [hep-ph/0108193].
- [21] T. Ota, J. Sato and N. -a. Yamashita, Phys. Rev. D **65**, 093015 (2002) [hep-ph/0112329].
- [22] M. Campanelli and A. Romanino, Phys. Rev. D **66**, 113001 (2002) [hep-ph/0207350].
- [23] M. Blennow, T. Ohlsson and W. Winter, Eur. Phys. J. C **49**, 1023 (2007) [hep-ph/0508175].
- [24] J. Kopp, M. Lindner and T. Ota, Phys. Rev. D **76**, 013001 (2007) [hep-ph/0702269 [HEP-PH]].
- [25] J. Kopp, M. Lindner, T. Ota and J. Sato, Phys. Rev. D **77**, 013007 (2008) [arXiv:0708.0152 [hep-ph]].
- [26] N. C. Ribeiro, H. Minakata, H. Nunokawa, S. Uchinami and R. Zukanovich-Funchal, JHEP **0712**, 002 (2007) [arXiv:0709.1980 [hep-ph]].
- [27] A. Bandyopadhyay *et al.* [ISS Physics Working Group Collaboration], Rept. Prog. Phys. **72**, 106201 (2009) [arXiv:0710.4947 [hep-ph]].
- [28] N. C. Ribeiro, H. Nunokawa, T. Kajita, S. Nakayama, P. Ko and H. Minakata, Phys. Rev. D **77**, 073007 (2008) [arXiv:0712.4314 [hep-ph]].
- [29] J. Kopp, T. Ota and W. Winter, Phys. Rev. D **78**, 053007 (2008) [arXiv:0804.2261 [hep-ph]].
- [30] M. Malinsky, T. Ohlsson and H. Zhang, Phys. Rev. D **79**, 011301 (2009) [arXiv:0811.3346 [hep-ph]].
- [31] A. M. Gago, H. Minakata, H. Nunokawa, S. Uchinami and R. Zukanovich Funchal, JHEP **1001**, 049 (2010) [arXiv:0904.3360 [hep-ph]].
- [32] OPERA collaboration, M. Guler et al., (2000), CERN-SPSC-2000-028.
- [33] R. Antolini, (ed.), (Gran Sasso) “INFN LNGS - Laboratori Nazionali del Gran Sasso. Annual report 2010,” LNGS-EXP-01-11.
- [34] M. C. Gonzalez-Garcia, Y. Grossman, A. Gusso and Y. Nir, Phys. Rev. D **64**, 096006 (2001) [hep-ph/0105159].

- [35] D. Delepine, V. G. Macias, S. Khalil and G. Lopez Castro, Phys. Rev. D **79**, 093003 (2009) [arXiv:0901.1460 [hep-ph]].
- [36] C. Biggio, M. Blennow and E. Fernandez-Martinez, JHEP **0908**, 090 (2009) [arXiv:0907.0097 [hep-ph]].
- [37] K. Ikado *et al.*, Phys. Rev. Lett. **97**, 251802 (2006) [arXiv:hep-ex/0604018].
- [38] U. Nierste, S. Trine and S. Westhoff, Phys. Rev. D **78**, 015006 (2008) [arXiv:0801.4938 [hep-ph]].
- [39] K. Kiers, K. Little, A. Datta, D. London, M. Nagashima and A. Szykman, Phys. Rev. D **78**, 113008 (2008) [arXiv:0808.1707 [hep-ph]]; A. Datta, K. Kiers, D. London, P. J. O'Donnell and A. Szykman, Phys. Rev. D **75**, 074007 (2007) [Erratum-ibid. D **76**, 079902 (2007)] [hep-ph/0610162].
- [40] N. Agafonova *et al.* [OPERA Collaboration], Phys. Lett. B **691**, 138 (2010) [arXiv:1006.1623 [hep-ex]]. R. Acquafredda *et al.* [OPERA Collaboration], New J. Phys. **8**, 303 (2006) [hep-ex/0611023].
- [41] D. Meloni and M. Martini, arXiv:1203.3335 [hep-ph].
- [42] T. Teshima and T. Sakai, Analysis of atmospheric neutrino oscillations in three flavor neutrinos, Phys. Rev. D **62**, 113010 (2000) [hep-ph/0003038].
- [43] M. C. Gonzalez-Garcia, M. Maltoni and J. Salvado, JHEP **1004**, 056 (2010) [arXiv:1001.4524 [hep-ph]].
- [44] F. P. An *et al.* [DAYA-BAY Collaboration], arXiv:1203.1669 [hep-ex].
- [45] C. H. Llewellyn Smith, Phys. Rept. **3**, 261 (1972). S. K. Singh and E. Oset, Phys. Rev. C **48**, 1246 (1993). A. Strumia and F. Vissani, Phys. Lett. B **564**, 42 (2003) [astro-ph/0302055]. T. Goringe and H. W. Fearing, Rev. Mod. Phys. **76**, 31 (2004) [nucl-th/0206039].
- [46] O. Deschamps, S. Descotes-Genon, S. Monteil, V. Niess, S. T'Jampens and V. Tisserand, Phys. Rev. D **82**, 073012 (2010) [arXiv:0907.5135 [hep-ph]].
- [47] See, e.g., R. A. Diaz, hep-ph/0212237, O. Deschamps, S. Descotes-Genon, S. Monteil, V. Niess, S. T'Jampens and V. Tisserand, Phys. Rev. D **82**, 073012 (2010) [arXiv:0907.5135 [hep-ph]], G. C. Branco, P. M. Ferreira, L. Lavoura, M. N. Rebelo, M. Sher and J. P. Silva, arXiv:1106.0034 [hep-ph].
- [48] M. Davier, A. Hocker and Z. Zhang, Rev. Mod. Phys. **78**, 1043 (2006) [hep-ph/0507078].

- [49] B. C. Barish, In *Stanford 1989, Proceedings, Study of tau, charm and J/psi physics* 113-126 and Caltech Pasadena - CALT-68-1580 (89,rec.Oct.) 14 p
- [50] K. Nakamura et al. (Particle Data Group), J. Phys. G 37, 075021 (2010) and 2011 partial update for the 2012 edition.
- [51] Z. G. Wang and S. L. Wan, Phys. Rev. C **76**, 025207 (2007) [hep-ph/0607135].
- [52] A. A. Aguilar-Arevalo et al. [MiniBooNE Collaboration], Phys. Rev. D 81 (2010) 092005.
- [53] T. Gorringer and H. W. Fearing, Rev. Mod. Phys. **76**, 31 (2004) [nucl-th/0206039].
- [54] K. S. Kuzmin, V. V. Lyubushkin and V. A. Naumov, Eur. Phys. J. C **54**, 517 (2008) [arXiv:0712.4384 [hep-ph]].